Coanda effect enhanced air assisted flare for low flow operation: cold flow CFD analysis

Ahmed A. Maaroof [1], Joseph D. Smith [2] and Mohammed H. S. Zangana [3]

[1] Petroleum Eng.Dept., Koya Univ, Kurdistan Region – F.R. Iraq, ahmed.maaroof@koyauniversity.org

[2] Chem and Biochem Eng, Laufer Endowed Energy Chair, Missouri Univ of Sci and Tech, USA, smithjose@mst.edu

[3] Petroleum Eng.Dept., Koya Univ, Kurdistan Region – F.R. Iraq, mohammed.zangana@koyauniversity.org

Abstract

This paper aims at increasing the flow velocity in the flare stack by decreasing the flow diameter to solve the issue of low flow operation in the flares. A new air assisted flare design of 1m height and 15cm diameter has been tested using CFD simulation in this work. The design includes injecting air at different velocities (0.6m/s, 0.8m/s and 1m/s) from small pipes added near the tip of the flare to produce thrust to increase the stack cross velocity like in aircrafts during the takeoff. Moreover, to produce homogenous distribution of air from pipes and direct it toward the cross flow in the stack, a curved surface has been added to the design in front of pipes' exit to produce Coanda effect and to ensure a homogenous mixing with cross flow in the stack. Furthermore, a cone has been added to the design above the small pipes to ensure the flow will be directed to the tip of the flare. In this work, C3D CFD code based on LES has been used to study the effect of Coanda principle using cold flow approach in three different cases. In this simulation, the total number of hexahedral cells were 1222100 (110*110*101), with aspect ratio and growth ratio of 1. Three cases have been applied in this work, injecting air through the slots at three different velocities in each case; 0.6m/s, 0.8m/s and 1m/s while keeping the injection velocity of the air through the stack constant at each case at 0.78m/s. Ten vertical locations at the centre of the stack have been chosen to measure the cross flow velocity in the stack. The results showed that as the pipes' flow velocity increase, the cross velocity increases due to decreasing flow diameter. Highest velocity of the cross flow measured equal to 1.83m/s, during 1m/s injection from each slot above the tip at 1.05m. finally, at the same location, cross flow velocity measured to be 1.25m/s in case of 0.6m/s injection from each slot, and 1.51m/s in case of 0.8m/s injection from each slot.

Introduction

Generally, flares are safety devices designed to burn either large volumes of gases during start-up or shut-down process, or small amount of gases during routine operation (Torres et al., 2012; Bader, Baukal and Bussman., 2011). Field observations indicated that high combustion efficiencies achieved at high flow condition (McDaniel and Tichenor.,1983; Pohl et al., 1986) while low combustion efficiencies below 98-99% observed by some field measurements at low flow conditions (Strosher., 2000; Mellqvist., 2001; Cade and Evans., 2010; Ewing, Roesler and Evans., 2010). Studies showed that there are several factors cause low combustions efficiencies at low flow conditions. For example, velocity of vent gas and flammability of the vent gas mixture (Torres et al., 2012).

Recently, a study by Alhameedi et al., (2021) tested a new air-assisted flare that designed to increase the low flowrate of waste gas and increase the mixing by adding radial slots near the tip. Injecting air from radial slot was to control the exit area in order to increase the axial flow velocity; thus, increasing the mixing between the gas and surrounding air to achieve better combustion efficiency during low flow operations.

Furthermore, the principle of injecting a jet into the crossflow observed in many applications; for example, combustion equipment, mixing tanks, quenching systems and drying systems. the distribution of flow in the domain of crossflow reported affected by many factors including jet geometry, jet exhaust velocity and the characteristics of the crossflow and injecting fluids (Alhameedi et al., 2021), where both computational and experimental approaches have been used to study the effects of different factors on the flow properties of jet gas injected into crossflow (Liscinsky, True and Holdeman, 1996; Kartaev et al., 2018; Elattar, Fouda and Bin-Mahfouz, 2016; Kartaev et al., 2014; Nada, Fouda and Elattar, 2016).

In 1910, the Coanda effect was observed for the first time by Henri Coanda (engineer and mathematician) (Coanda., 1932; Reba, 1966), when air ejected from a rectangular nozzle observed to attached to an inclined flat plate that connected to the nozzle's output. In fact, Coanda effect observed needs to a sharp angle between the flat plate and nozzle; and therefore, a series of tests have been conducted using deflecting surfaces each at different angle. These attempts succeeded in changing the flow direction through angles as large as 180° (Lubert, 2010).

Generally, Henri explained the Coanda effect as “when a jet of fluid is passed over a curved surface, it bends to follow the surface, entraining large amounts of air as it does so". In other words, The Coanda effect can be defined as the tendency of a fluid to attached to a nearby surface and stay attached to it even if the surface curves away from the direction of initial jet (Wille and Fernholz., 1965).

In some cases, it has been observed that the Coanda effect represented by curved surface can entrain up to twenty times of jets volume when passed through (Parsons., 1990). Coanda principle can be found in various natural and man-made examples (such as medicine, industrial processes, maritime technology, and aerodynamics) due to the improvement in turbulent levels and entrainment (Lubert, 2010; Wille and Fernholz., 1965). On the other hand, the major problem of Coanda effect is detachment of the jet flow due to high static pressure at the nozzle exit. Therefore, to prevent or delay this problem is through reducing the static pressure at the nozzle exhaust. For example, using a convergent-divergent nozzle can significantly lower the static pressure and solve the problem (Carpenter and Green, 1997).

In the petroleum industry, the Coanda principle has been used to improve flare operation by designing Coanda flares (Castaneda and Valera-Medina, 2019). Due to the fact that Coanda effect entrain large amount of air, this kind of flares compared to other types produce higher combustion efficiency, better smokeless operation and less thermal radiation (Desty, Boden and Witheridge., 1978). Furthermore, the Coanda principle has been also used in aircraft for thrust vectoring for short take-off and landing (Valera-Medina and Baej, 2016).

The current study focus on increasing the thrust in a new air-assisted flare design by reducing the cross sectional area of the flow in the stack and thus increasing the velocity (see equation 1). The proposed idea includes adding small pipes around the stack near the tip. The design also includes adding a curved surface inside the stack and in front of small pipes to produce homogenous flow from all directions toward the cross flow in the stack. The study also tests the effect of changing flow velocity from slots (small pipes) on the cross flow velocity in the stack. Figure (1) shows the direction of the flow from pipes and stack, and figure (2) shows the dimensions of the flare in a 3D model made using solidworks software.

$$tip\ velocity = \frac{m}{\rho S}\ \ where\ S = \frac{\pi D_{nozzle}^2}{4} \qquad \text{Equation 1}$$

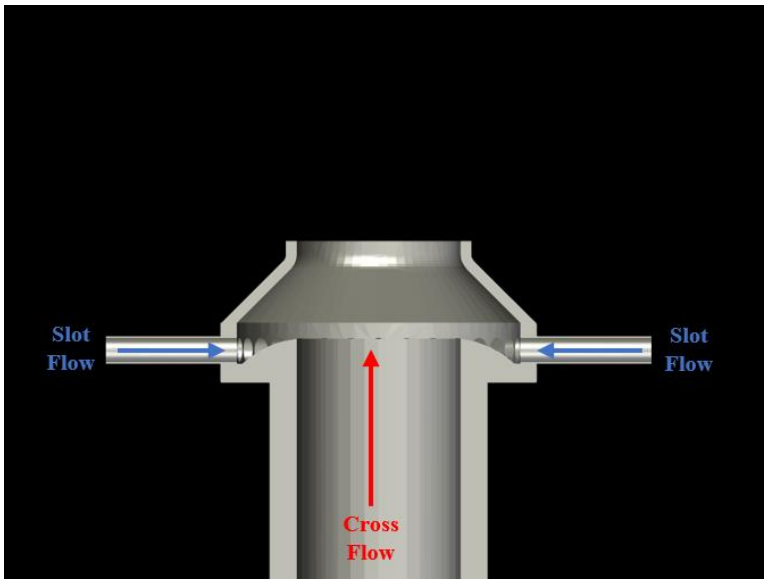

Figure 1: flow directions in the stack

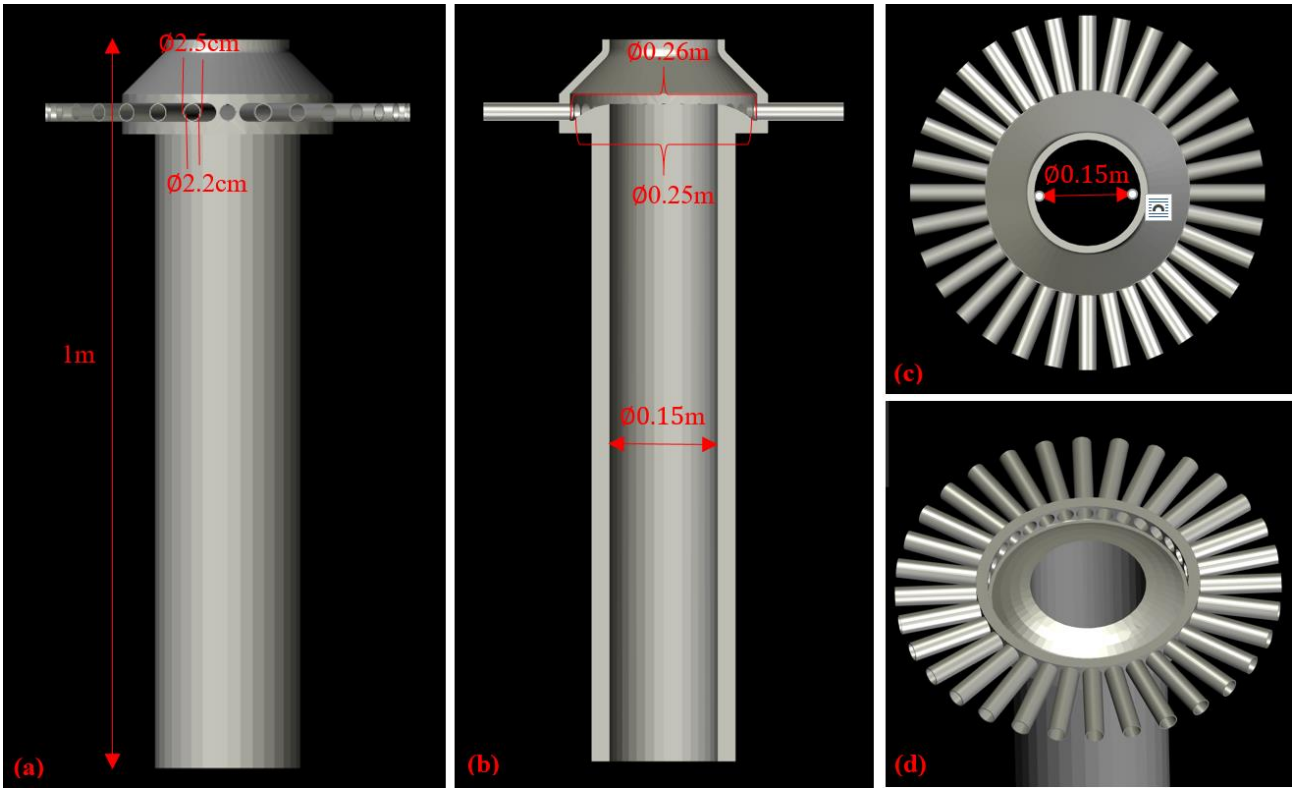

Figure 2: Flare dimensions and details; (a) side view of the flare, (b) cross-section view of the flare, (c) top view, (d) flare without the cone view.

Computational Fluid Dynamics Models

In this study, C3D LES based Computational Fluid Dynamics (CFD) code version 6-8-22 has been used to simulate the effect of Coanda surface on mixing between air flow from small pipes (slots) and cross flow in the stack. In this simulation, three cases of air velocities have been applied. These include injecting air at three different velocities of 0.6m/s, 0.8m/s and 1m/s from each slot (pipe), while the cross air flow in the stack has been kept constant at 0.78m/s in all three cases.

In this simulation, the governing equations discretized using finite volume approach with orthogonal Cartesian coordinates to makes the discretization very similar to a finite difference approach. All vector quantities in a finite volume formulation such as momentum is defined at the cell interface and scalar variables such as pressure and temperature are defined at cell centers. The flow equations in C3d code solved using a compressible version of the PISO (Issa, 1986) pressure based solution algorithm (Suo-Anttila, 1993). Furthermore, Large Eddy Simulation (LES) formulation used to modeling turbulence. In this simulation, used air is assumed to be incompressible with slight changes in temperatures. Moreover, the momentum equation used in this simulation is solved using conservative form of the momentum flux vector ($\rho \boldsymbol{u}$).

$$\frac{\partial \rho \mathbf{u}}{\partial t} + [\nabla \bullet \mathbf{u}\, \rho \mathbf{u}] = -\nabla P - \rho \mathbf{u} F + \nabla(\mu + \rho\varepsilon)\nabla \mathbf{u} + \rho \mathbf{g}$$

The energy equation used in this simulation is solved using the equation below.

$$\frac{\partial \rho c_p T}{\partial t} + \nabla \bullet \rho c_p \mathbf{u} T = \nabla \bullet (k + \rho c_p \varepsilon)\nabla T + \Sigma h_s \frac{A_s}{V}(T_s - T) + Q_V + \frac{1}{\gamma}\frac{DP}{Dt} - \frac{1}{2}\left[\frac{\partial}{\partial t}(\rho u^2) + \nabla \bullet \rho \mathbf{u} u^2\right]$$

Computational Domain & Flare Model

The computational domain size used in this work were 2m height, 2m length and 2m width. The height of the domain is on z-axis and started from – 0.1 to 0 to specify a ground for the flare model, then from zero to 2m. the length of the domain is on x-axis and started from – 1m to +1m. Finally, the width defined on y-axis and started from – 1m to +1 m. Both x-axis and y-axis start from – 1m to +1m to define a center to locate the flare model. The flare model dimensions used in the simulation were 1m height and 0.15m inside diameter. Figure (3) shows the domain and flare computational mesh and size.

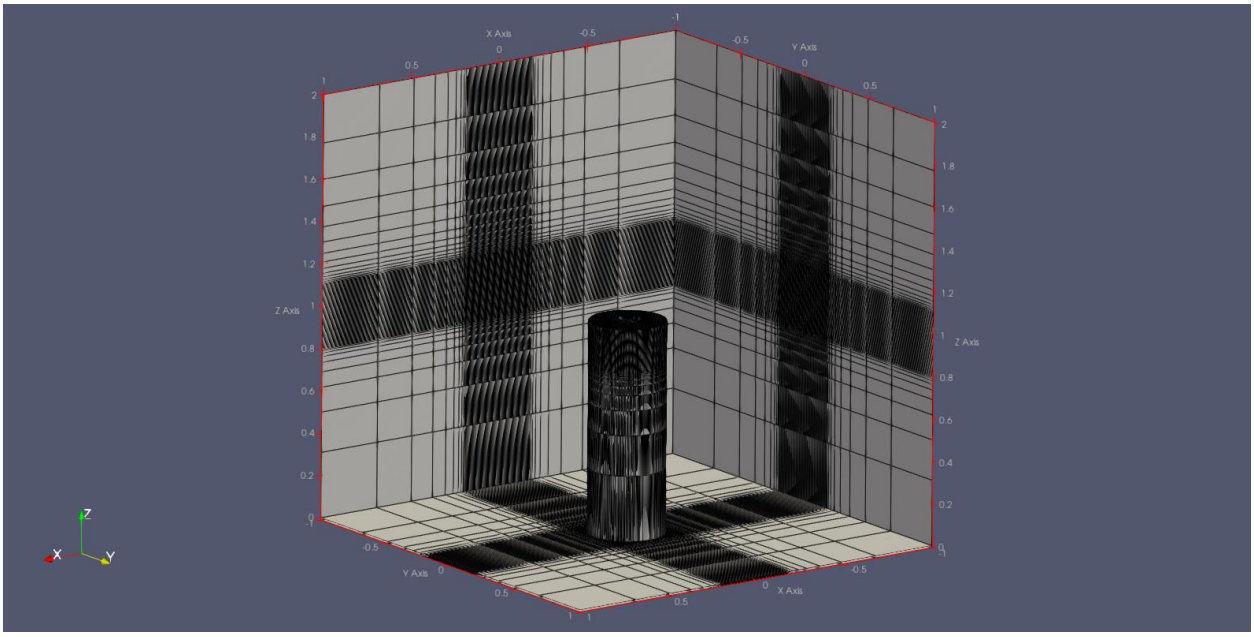

Figure 3: Flare CFD Model and the domain mesh and size

The flare model built using C3D code modeler by first using a solid cylinder of length 1m and diameter of 0.36m then a hollow cylinder of diameter of 0.15m and length of 1m has been added to define flare inside diameter of the stack. To add Coanda effect, near the tip between 0.8875m and 0.9125m, a curved surface using half elliptical sphere of diameter of 0.25m and height of 0.025m has been added to the model. Furthermore, between 0.889m and 0.911m, a short hollow cylinder of diameter of 0.15m has been defined to allow to locate the slot injectors at height of 0.9 m and a diameter of 0.26 m. Each injector has been defined to have a diameter of 2.2cm which is the inside diameter of the slots. The maximum allowable number of pipes (slots) were 32 pipes (slots) of inside and outside diameters 2.2cm and 2.5cm respectively. This number of slots has been calculated by dividing the perimeter of the stack at the point where the slot injection happens (0.26m) by the outside diameter of the pipes (0.025m). Finally, from 0.92m till the end of the stack, a hollow cone of diameters 0.26m and 0.15m has been added to give more control for the thrust.

The total number of hexahedral cells were 1222100 (110*110*101), and it were very fine in the area between 0.8m and 1.1m with 607500 hexahedral cells (90*90*75) (see figure 4) to capture the effect of Coanda surface on flow from small slots, the mixing between slots flow and cross flow; as well as, to measure the change in the air velocity in the stack. The aspect ratio and growth ratio at the area of interest which is between 0.8m and 1.1m were near to 1, with cell size dx=dy=dz= 4mm. The grid has been refined using higher number of cells to better capture the

velocity changes in the stack and to confirm that the 1222100 cell simulation was sufficiently accurate. Figure (5) show the mesh independence study for case 1m/s air injection in each slot. The results showed that 1222100 cell and 1569600 cell (120*120*109) give almost the same trend unlike 727904 cell (92*92*86), where less velocity measured in the stack.

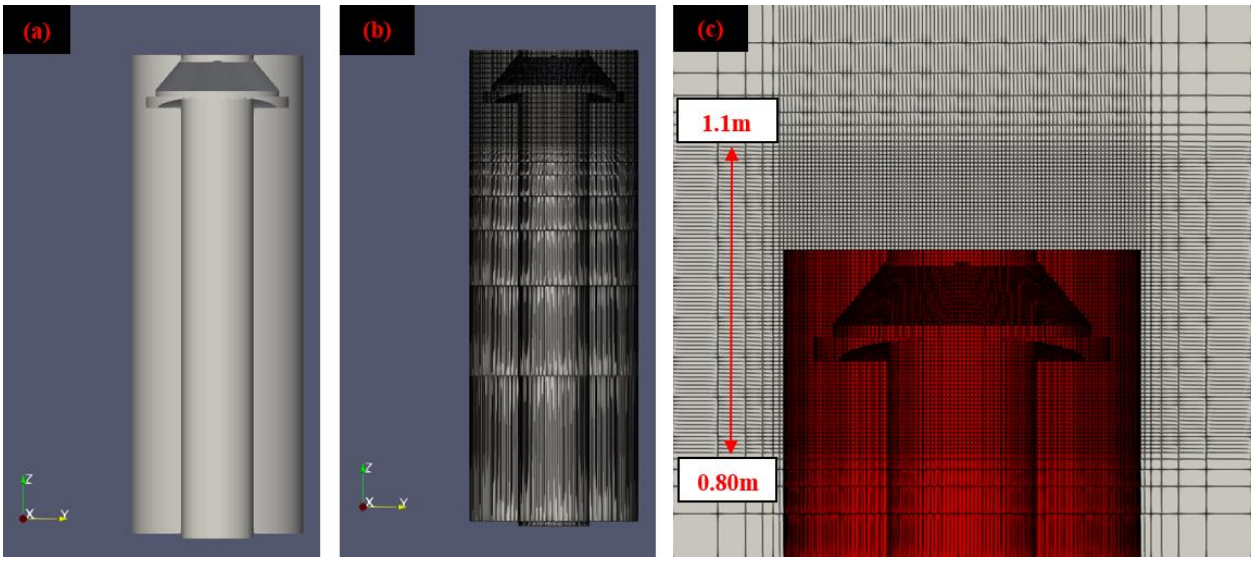

Figure 4: Different cross-sectional views of the Flare model built by C3d code modeler. (a) solid view, (b) model meshing, (c) meshing in the area of interest 0.8m and 1.1m.

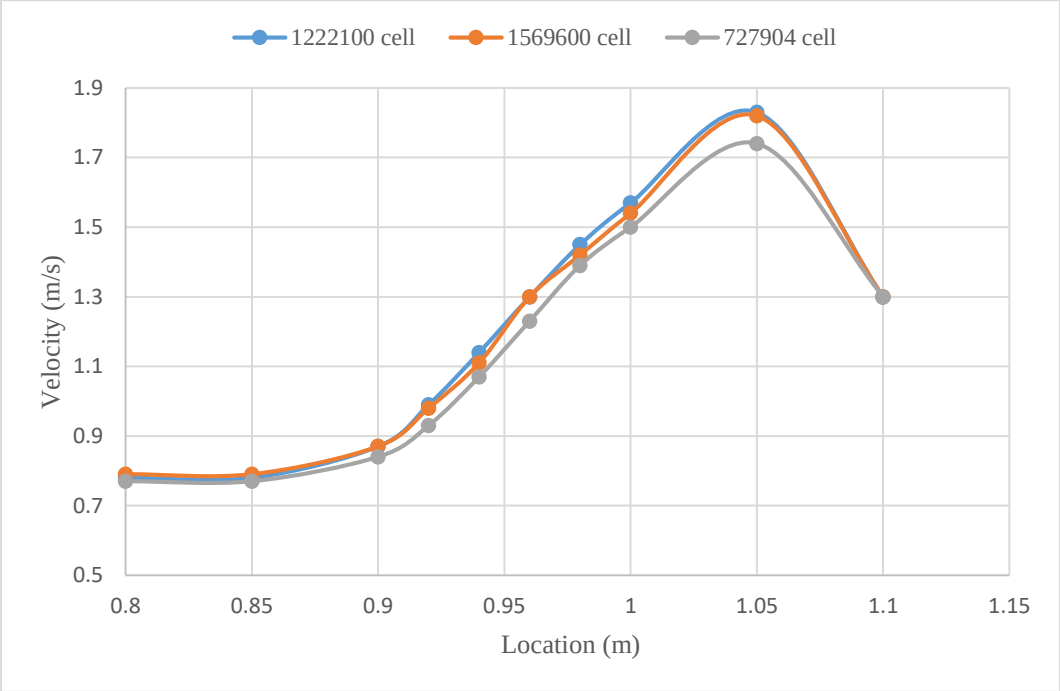

Figure 5: Mesh Independence study for case 1m/s injection from slots

Boundary conditions

The boundary conditions used in this simulation included a no wind or cross wind blowing from x-axis or y-axis on the flare model. Also, the boundary conditions included defining hydrostatics pressure at 294 k across the domain. 1-d sub grid has been defined for slots injectors (small pipes surrounding the main stack) to allow to define the injector in the model and also to control the changing in the flow rate of the air through each injector. The ground of the domain has been defined as dry sand, and steel carbon has been selected as a material for the stack model. In this simulation cold flow test approach has been applied which means only air is used as a fluid flow in both stack and small pipes. The flow rate and temperature of the air through the flare stack have been defined to 0.78m/s and 305k, and the exit of the flare to 3-D pressure. Moreover, the flow rate the air flowing through each slot in the three cases have been set to 0.6m/s, 0.8m/s and 1m/s, at 310K and the exit of the flare to 3-D pressure.

Post Processing and Transient Calculation

At the beginning, the simulation run for 100 timesteps to calibrate the air mass flow rate injected through the stack and small pipes. After this step, the simulation timesteps and time set to 10000 step and 10 second respectively to allow the process stabilize. Figure (6) shows the simulations reach stability at $1.5*10^{-5}$ second in all three cases.

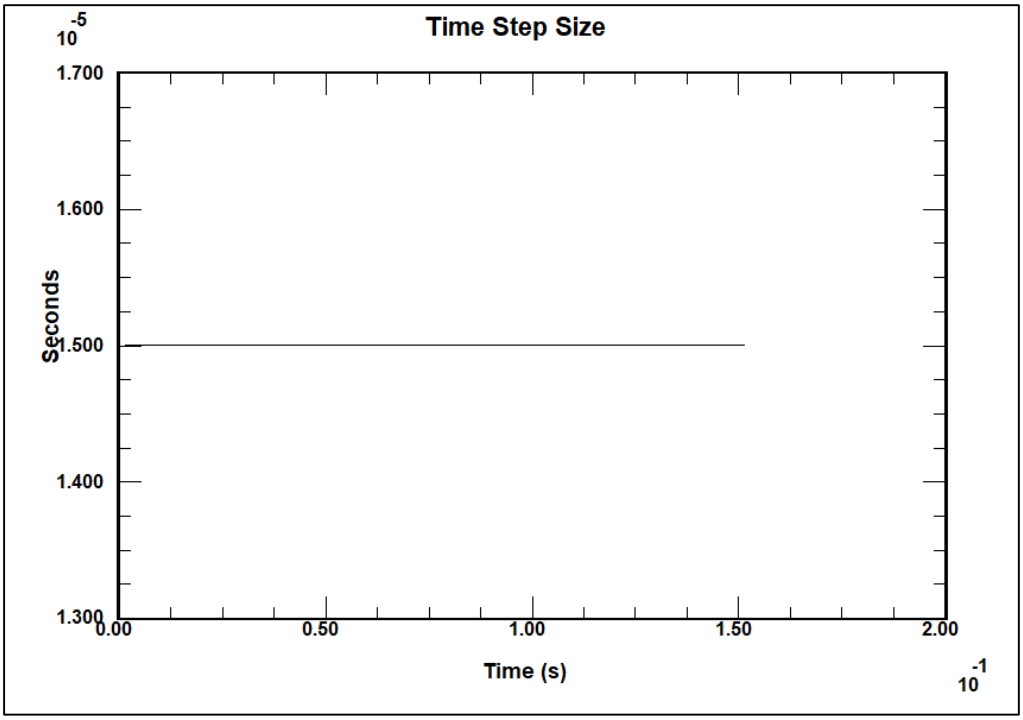

Figure 6: Simulation run stability

Results

Paraview version 5.10.0 has been used to visualize the effect of Coanda surface on flow from the 32 slots around the main stack. Furthermore, Paraview has been used to measure the velocity of the air in the center of the stack at ten different locations using probe option. Figure (7) shows the location of the probes used to measure the velocity at ten different vertical positions in the stack. Furthermore, table (1) shows the coordinates of the probes along with the increase of the air velocity in stack as a result of increasing flow velocity from slots.

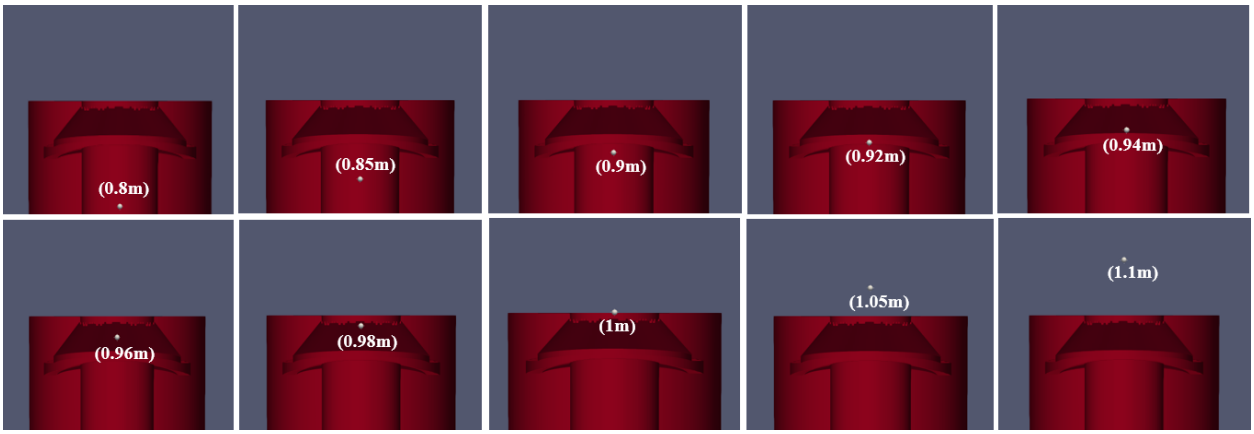

Figure 7: Location of the probes

Table 1: probe coordinates along with cross flow velocity in the stack

Probe Coordinates			Case 1 (0.6m/s)	Case 2 (0.8m/s)	Case 3 (1m/s)
x-axis (m)	y-axis (m)	z-axis (m)			
0	0	0.80	0.78	0.78	0.78
0	0	0.85	0.78	0.78	0.78
0	0	0.90	0.83	0.86	0.87
0	0	0.92	0.89	0.95	0.99
0	0	0.94	0.98	1.07	1.14
0	0	0.96	1.10	1.20	1.30
0	0	0.98	1.20	1.32	1.45
0	0	1.00	1.28	1.44	1.57
0	0	1.05	1.25	1.51	1.83
0	0	1.10	0.76	1.01	1.30

In each case, a temperature plane made in Paraview to visualize the flow shape and direction from slots. These planes showed that the curved surface directed the slots flow to decrease the flow area of the cross flow. Figure (8) shows the effect of increasing flow from slots on decreasing the flow diameter in the stack.

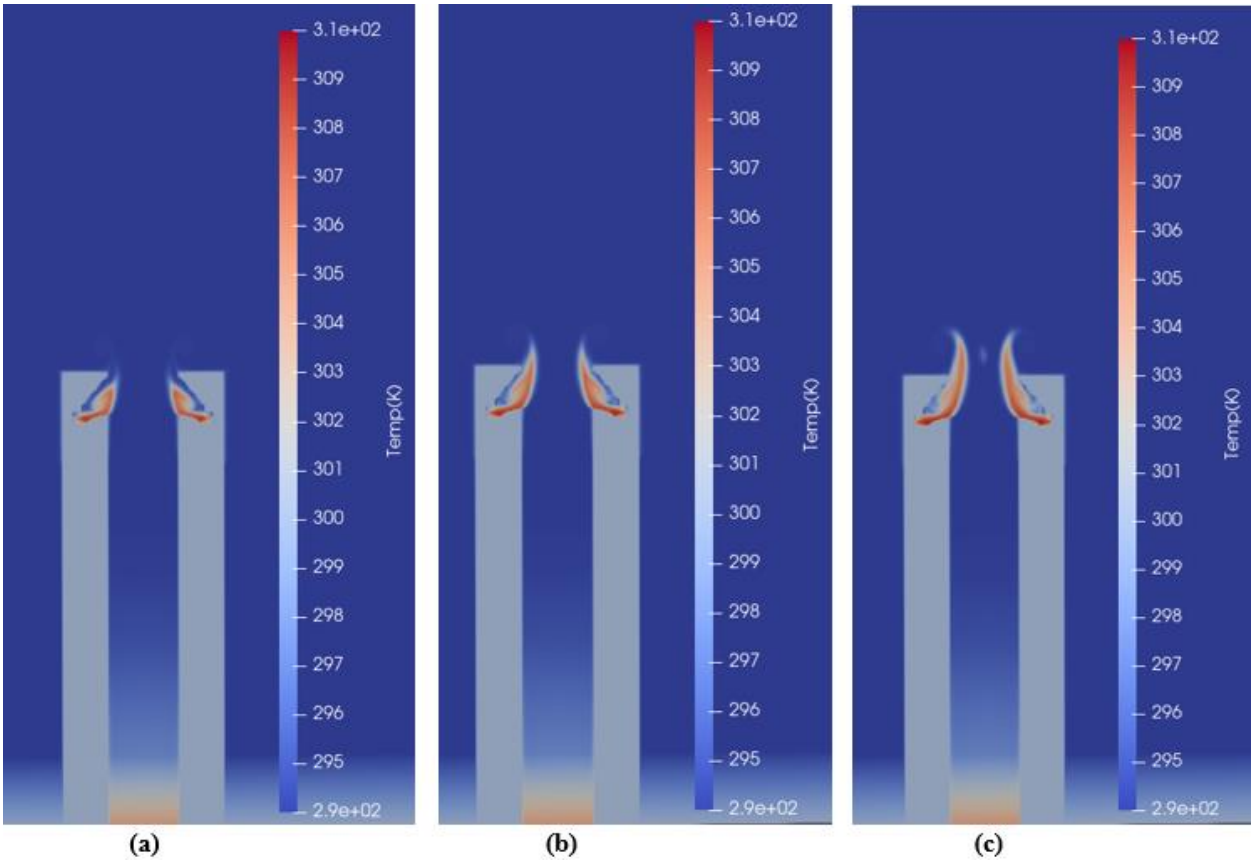

Figure 8: Temperature Planes; (a) 0.6m/s from each slot, (b) 0.8m/s from each slot, (c) 1m/s from each slot.

Furthermore, according to figure (9), as the slot velocity increases the cross flow increases due to decreasing the flow diameters. According to this figure, in the three cases, the stack velocity measured to be almost the same 0.78m/s in the (z-axis) locations 0.8m and 0.85m due to the fact that these two positions are located below the Coanda surface. On the other hand, it is clear that in the positions where the Coanda surface start slightly above 0.9m, the stack velocity increase significantly until slightly higher than the tip of the stack. For example, in the case of 1m/s air flow from each slot, the highest increase in the stack velocity is measured at 1.05m with 1.83m/s cross flow velocity. Moreover, in case of 0.8m/s air flow in the slots, the highest velocity is measured near to 1.05m with 1.51m/s, while in the case of 0.6m/s, the highest velocity is recorded at the tip of the stack (1m) with 1.28m/s. Regardless, in the all three cases, the stack velocity reached the peak a point then starts to decrease, still the lowest velocity measured in case 2 (0.8m/s) and case 3 (1m/s) is higher than the injection velocity in the stack 0.78m/s. For example, in the position 1.1m, the stack velocity in the case 3 is 1.30m/s which is significantly higher the 0.78m/s (air velocity in the stack). These results showed that as the slots velocity increase, the velocity of the

cross flow in the stack increase due to increasing thrust caused by decreasing the flow diameter and area.

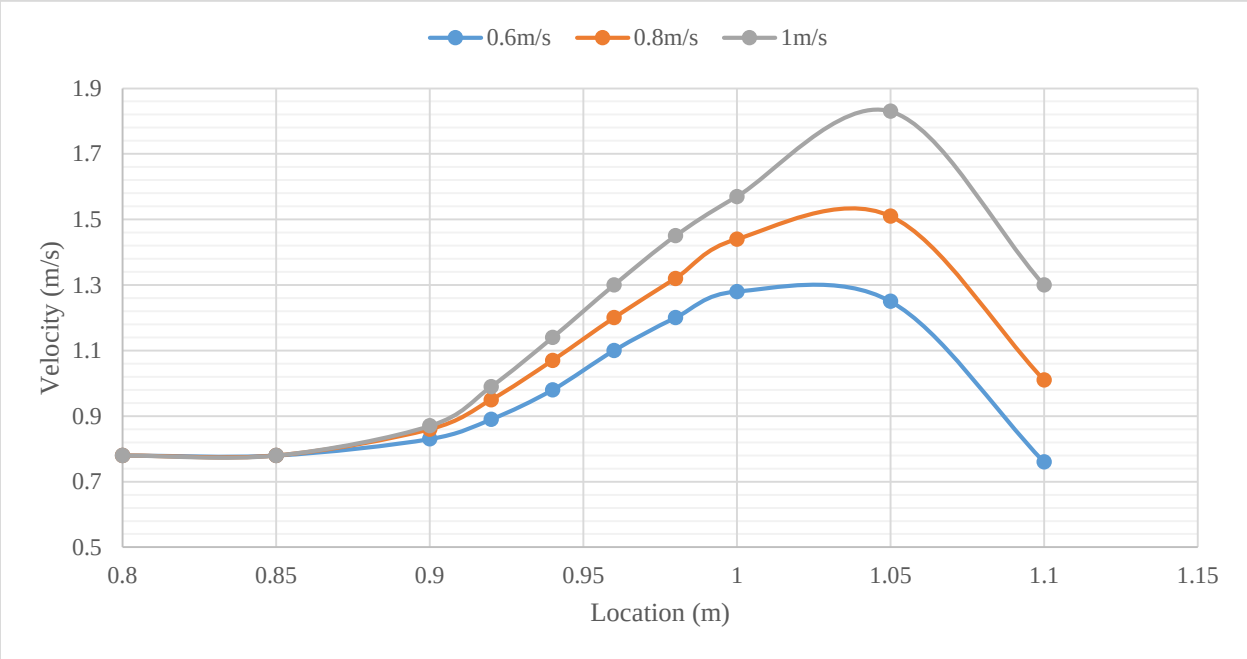

Figure 9: Cross flow velocity at different locations

Conclusion

This study investigated the effect of using Coanda principle in a new air assisted flare design to increase the flow velocity of low flow operation flares. The design includes 32 small pipes of diameters 2.2cm ID and 2.5cm OD have been added around the tip of a stack of 15cm ID and 1m height. Furthermore, near the tip of flare, the design included; a curved surface of diameters 25cm and 15cm, and height of 2.2cm; as well as, a cone of diameters 26cm and 15cm. CFD code C3D based on LES simulation has been used to investigate the cold flow operation (injecting air in both pipes and the stack) of the design. Three cases have been applied in the simulation; case 1, injecting air at 0.6m/s through each pipe; case 2, injection air at 0.8m/s through each pipe; finally, injecting air at 1m/s through each pipe. In all three cases, the air flow in the stack kept constant at 0.78m/s. The simulation carried out with no cross wind blowing from sides toward the stack. Finally, 1222100 hexahedral cell have been used in the simulation with aspect ratio and growth ratio of 1. Furthermore, Paraview software has been used to visualize the simulation flow shape and direction, as well as measuring the cross flow velocity in the stack at different locations. Ten vertical locations (on z-axis) have been defined to measure the cross velocity in the stack. The

results showed that the Coanda effect worked efficiently by directing the pipes flow upward and avoid spreading it downward in the stack. Furthermore, the Coanda effect produced a homogenous distribution of the pipes' flow and decrease the cross flow diameter in the stack resulting in increasing the velocity. In the three cases, the peak of cross velocity reached at the tip of the stack in the locations between 1m and 1.05m, after that the velocity started to decrease slightly. However, the velocity measured after the peak still observed higher than the injection velocity of 0.78m/s in most cases. The highest velocity of the cross flow in the stack measured in the case of injecting 1m/s air in the small pipes, while the lowest velocity measure in the case of 0.6m/s air flow in the small pipes.

References

Alhameedi, H.A., Hassan, A.A., Smith, J.D. and Al-Dahhan, M., 2021. Toward a Better Air-Assisted Flare Design for Purge Flow Conditions: Experimental and Computational Investigation of Radial Slot Flow into a Crossflow Environment. *Industrial & Engineering Chemistry Research*, *60*(6), pp.2634-2641.

Bader, A., Baukal, C.E. and Bussman, W., 2011. Selecting the proper flare systems. *Chemical Engineering Progress*, *107*(7), pp.45-50.

Castaneda, V. and Valera-Medina, A., 2019. Coanda flames for development of flat burners. *Energy Procedia*, *158*, pp.1885-1890.

Cade, R. and Evans, S., 2010. Performance test of a steamassisted elevated flare with passive FTIR. *Chicago, Illinois: Clean Air Engineering*.

Carpenter, P.W. and Green, P.N., 1997. The aeroacoustics and aerodynamics of high-speed Coanda devices, part 1: Conventional arrangement of exit nozzle and surface. *Journal of Sound and Vibration*, *208*(5), pp.777-801.

Coanda, H., 1932. Procédé de propulsion dans un fluide. *Brevet Invent. Gr. Cl*, *2*.

Desty, D.H., Boden, J.C. and Witheridge, R.E., 1978. The origination, development and application of novel premixed flare burners employing the Coanda effect, 85th Nat. In *AIChE meeting, Philadelphia*.

Elattar, H.F., Fouda, A. and Bin-Mahfouz, A.S., 2016. CFD modelling of flow and mixing characteristics for multiple rows jets injected radially into a non-reacting crossflow. *Journal of Mechanical Science and Technology*, *30*(1), pp.185-198.

Ewing, B., Roesler, D. and Evans, S., 2010. Performance Test of a Steam-Assisted Elevated Flare with Passive FTIR-Detroit. Final Report. Detroit: Marathon Petroleum Company, LP & Clean Air Engineering.

Issa, R.I., 1986. Solution of the implicitly discretised fluid flow equations by operator-splitting. *Journal of computational physics*, *62*(1), pp.40-65.

Kartaev, E.V., Emelkin, V.A., Ktalkherman, M.G., Aulchenko, S.M. and Vashenko, S.P., 2018. Upstream penetration behavior of the developed counter flow jet resulting from multiple jet impingement in the crossflow of cylindrical duct. *International Journal of Heat and Mass Transfer*, *116*, pp.1163-1178.

Kartaev, E.V., Emel'Kin, V.A., Ktalkherman, M.G., Kuz'Min, V.I., Aul'Chenko, S.M. and Vashenko, S.P., 2014. Analysis of mixing of impinging radial jets with crossflow in the regime of counter flow jet formation. *Chemical Engineering Science*, *119*, pp.1-9.

Lubert, C., 2010, November. On some recent applications of the Coanda effect to acoustics. In *Proceedings of Meetings on Acoustics 160ASA* (Vol. 11, No. 1, p. 040006). Acoustical Society of America.

Liscinsky, D.S., True, B. and Holdeman, J.D., 1996. Crossflow mixing of noncircular jets. *Journal of propulsion and power*, *12*(2), pp.225-230.

Mellqvist, J., 2001. Flare testing using the SOF method at Borealis Polyethylene in the summer of 2000. *Chalmers University of Technology. http://www. fluxsense. se/reports/flare paper final*, *201004*.

McDaniel, M. and Tichenor, B.A., 1983. Flare efficiency study.

Nada, S.A., Fouda, A. and Elattar, H.F., 2016. Parametric study of flow field and mixing characteristics of outwardly injected jets into a crossflow in a cylindrical chamber. *International Journal of Thermal Sciences*, *102*, pp.185-201.

Parsons, C., 1990. An experimental and theoretical study of the aeroacoustics of external-Coanda gas flares.

Pohl, J.H., Tichenor, B.A., Lee, J. and Payne, R., 1986. Combustion efficiency of flares. *Combustion science and technology*, *50*(4-6), pp.217-231.

Reba, I., 1966. Applications of the Coanda effect. *Scientific American*, *214*(6), pp.84-93.

Strosher, M.T., 2000. Characterization of emissions from diffusion flare systems. *Journal of the Air & Waste Management Association*, *50*(10), pp.1723-1733.

Suo-Anttila, A., 1993. *F2D user's manual: A two-dimensional compressible gas flow code* (No. SAND-92-7343). Sandia National Labs., Albuquerque, NM (United States); Science Applications International Corp., Albuquerque, NM (United States).

Torres, V.M., Herndon, S., Kodesh, Z. and Allen, D.T., 2012. Industrial flare performance at low flow conditions. 1. Study overview. *Industrial & engineering chemistry research*, *51*(39), pp.12559-12568.

Valera-Medina, A. and Baej, H., 2016. Hydrodynamics during the transient evolution of open jet flows from/to wall attached jets. *Flow, Turbulence and Combustion*, *97*(3), pp.743-760.

Wille, R. and Fernholz, H., 1965. Report on the first European Mechanics Colloquium, on the Coanda effect. *Journal of Fluid Mechanics*, *23*(4), pp.801-819.